Prerequisites for Geostatistics on Unstructured Grids

John G. Manchuk and Clayton V. Deutsch

Extending geostatistical algorithms for unstructured grids come with several requirements: grids must be discretized to account for the scale of grid elements, the heterogeneity within them, and in a way that is admissible to the upscaling processes that are used; discretization must provide a set of points that represent a constant scale, preferably a point scale; the number and style of a discretization should lead to no biases. Results show that tetrahedral refinements do not lead to a bias using arithmetic upscaling and that convergence depends on the variogram, distribution function and element volume. For facies, convergence depends on the proportion. Permeability fields with higher contrasts and large heterogeneity show higher residuals and this highlights the importance of unstructured grid design.

Introduction

A recent problem for geostatistics is application to populating unstructured grids, which have been under consideration for reservoir analysis for some time. One major challenge is dealing with the huge variation of scales involved across a set of unstructured grid elements. Accounting for reservoir structures, wells, and heterogeneity can result in elements ranging from less than a cubic meter to thousands of cubic meters in volume. An initial response to dealing with these scales and others describing the various sources of data was direct geostatistics – a few past CCG papers on the subject include (Pyrcz and Deutsch, 2002; Manchuk et al, 2004; and Leuangthong, 2004). The motivation was to avoiding transformation to Gaussian space. Problems with non-linear averaging through the transformation are eliminated and average covariances account for the shape and volume of elements and sample volumes. However, many unsolved issues exist: theory for the shape of conditional distributions from kriging does not exist; multivariate distribution models to account for correlations between variables have not been adequately implemented; the impact of numerically assessing average covariances on the condition of systems of equations has not been assessed; and theory for estimating physical quantities such as permeability at scales other than points is undeveloped.

Current practice is to generate a high resolution (fine) model on a structured grid and upscale the results to an unstructured (coarse) grid. This approach has a number of issues. The fine and coarse grids do not conform causing problems for upscaling, especially with unstructured elements smaller than the structured elements, which can occur near wells, leads to a poor representation of heterogeneity; related to the last issue, unstructured elements are all represented by varying numbers of structured elements, which may lead to a bias; and structured grids contain numerous geometrical characteristics which are suboptimal for flow based upscaling.

Structured discretization is not the optimal choice. Most numerical integration schemes such as the midpoint, trapezoid, and various Gauss-quadrature rules only involve integration points within and on the boundary of a region. Therefore, the new approach involves discretization resulting in conforming grids. In general, this can only be accomplished if the discretization is also unstructured.

Admissible Discretization

Discretization of an unstructured grid is identical to refinement used in many numerical methods. The purpose of refinement is to reduce error, be it the error of numerical integration, of a velocity field in CFD modeling or of some other quantity. An unstructured grid is discretized or refined ultimately for upscaling purposes, to acquire effective reservoir properties as parameters for flow simulation. Different refinement strategies will result in different upscaling error. Choosing which to use is dependent on the upscaling processes involved – the refinement must be admissible for these processes.

Upscaling properties that average arithmetically with scale would permit many refinement approaches. The constraining process is flow based upscaling for permeability. A refinement must obey the requirements of the flow simulation technique used in the upscaling process. If two point flux approximation (TPFA) is used, the refinement must form an orthogonal grid such as regular or PEBI grids. In the majority of cases, neither method will be possible: regular grids could not conform to complex

unstructured elements and maintain orthogonality and generating PEBI grids that conform is non-trivial. It is possible to generate a PEBI grid such that its dual tetrahedral grid conforms, but then the problem of resolving flow velocities along the unstructured element interfaces during upscaling resurfaces. If the multipoint flux approximation (MPFA) method is used, then simulation can be done directly on the dual tetrahedral grid. MPFA can also be applied to non-orthogonal structured grids; however, generating conforming structured refinements for an unstructured grid is also a non-trivial problem.

Tetrahedral grids are one of the few admissible discretizations for unstructured grids and existing flow simulation algorithms. Aside from the fact than tetrahedral grids are used in many facets of engineering, several advantages are: methods for generation have been developed (Si, 2006) and are accessible; grids are easily constrained to conform to unstructured elements; the quality of tetrahedral elements can be controlled and this is important for stability of flow simulation; and generation can be tied to reservoir properties and to error estimates to improve results. Other prerequisites are explained with reference to this grid structure.

Scale

Sample data involved in reservoir modeling involve several scales and unstructured grids introduce a huge range of element scales as well. Integrating only the multiscale sample data has been a long standing problem in geostatistics. This is magnified when considering unstructured grids. Fortunately, the process of refinement has an additional use other than to achieve upscaled properties. It removes the need to make estimates at the scale of unstructured elements, effectively removing that huge range of scales mentioned previously. There is an underlying assumption: estimates made on a refinement are point scale. For tetrahedral refinements, point scale estimates are made either at the barycentres as in Figure 1 or the vertices. Correctness of this assumption is covered in the following text.

Averaging a set of point scale barycentre estimates is similar to the midpoint integration rule where the underlying function is a random field of a reservoir property. Each barycentre samples the field at that location. This process can be described in terms of regularized variables (1): the arithmetic average of a random variable Z_ω with scale ω to obtain its equivalent Z_V at another larger scale, V. Equation (1) is the exact form of an arithmetic average, but for an unstructured grid and its tetrahedral refinement, V represents a grid element and ω a set of tetrahedron barycentres. Defining the volume of each tetrahedron as w_k, barycentre locations x_k, and number of tetrahedra n, the approximate integral for (1) is expressed as a finite sum (2). A one dimensional depiction is given in Figure 2.

$$Z_V = \frac{1}{V}\int_V Z_\omega(x)dx \tag{1}$$

$$Z_V = \frac{1}{V}\sum_{k=1}^{n} w_k \cdot Z_\omega(x_k) \qquad \sum_{k=1}^{n} w_k = V \tag{2}$$

Generating estimates using (1) achieves the same goals as direct geostatistics, which were identified in the introduction: point scale estimation does not suffer from transformation problems making Gaussian simulation possible and discretization accounts for the shape and volume of elements. It can be shown for Gaussian fields that the intended approach of direct simulation using average covariances gives the same result as averaging a set of point scale simulated values. This is important for showing that use of point scale estimates is consistent with geostatistical scaling theory. Consider a case where a Gaussian value is to be conditionally simulated based on N conditioning data to represent an unstructured grid element using average covariance, which is approximated by discretizing the element into n points. In (3), $\mathbf{y}$ is the vector of conditioning data, $\overline{y}_s$ is the simulated value, $\boldsymbol{\lambda}$ is the vector of kriging weights, $\overline{\mathbf{c}}$ is the vector of average covariances between data samples and the grid element, C_{11} is the covariance matrix between the conditioning data, and r is a zero mean random deviate with variance equal to (4). Here, $\overline{C}(V,V)$ is the average covariance of the element, which describes the variance at scale V.

$$\begin{aligned}\overline{y}_s &= \boldsymbol{\lambda}^T\mathbf{y} + r \\ &= \overline{\mathbf{c}}^T C_{11}^{-1}\mathbf{y} + r\end{aligned} \tag{3}$$

$$\sigma_r^2 = \overline{C}(V,V) - \boldsymbol{\lambda}^T\overline{\mathbf{c}} \tag{4}$$

Now consider representing the same element by simulating point scale values at each of the *n* points and averaging them as in (2). For simplicity, assume all values represent an equal fraction of *V*, i.e. $w_k = 1/n, k = 1,\ldots n$. To account for all covariances, the *LU* formalism is used. Covariances between all conditioning data and discretization points is expressed in (5) along with its *LU* decomposition, where C_{12} is the covariance between data and points and C_{22} is between points. A conditional realization for all *n* points is generated using (6), where $\mathbf{y}_s$ is the vector of simulated values and $\mathbf{r}$ is a vector of zero mean random deviates with unit variance. Computing the mean and variance of the mean of (6) recovers exactly (3) and (4) respectively and this is shown in (7). The first step replaces $C_{11}^{-1}\mathbf{y}$ by $\boldsymbol{\alpha}$ as in dual kriging and the expected value of $L_{22}\mathbf{r}$ is a zero vector since $\mathrm{E}\{L_{22}\mathbf{r}\} = L_{22}\,\mathrm{E}\{\mathbf{r}\} = \mathbf{0}$. Summation of C_{12} over *i* and multiplying by 1 / *n* gives the same average covariance vector in (3) and replacing $\boldsymbol{\alpha}$ with its original matrix vector product recovers the same kriging estimate. Computing the variance of the mean is a straightforward quadratic form expression of the variance of $\mathbf{y}_s$ shown in (8), where $\mathbf{d} = [1/n \ldots 1/n]^T$. These results are only applicable when no transformation is used and the variable being estimated averages arithmetically. The advantage of using the second approach is realized when transformations and non-linear averaging are involved.

$$C = \begin{bmatrix} C_{11} & C_{12} \\ C_{12}^T & C_{22} \end{bmatrix} \underset{LU}{=} \begin{bmatrix} L_{11} & 0 \\ A_{12} & L_{22} \end{bmatrix} \begin{bmatrix} U_{11} & B_{12} \\ 0 & U_{22} \end{bmatrix} \tag{5}$$

$$\mathbf{y}_s = C_{21}C_{11}^{-1}\mathbf{y} + L_{22}\mathbf{r} \tag{6}$$

$$\begin{aligned} \mathrm{E}\{\mathbf{y}_s\} &= \mathrm{E}\{C_{21}C_{11}^{-1}\mathbf{y}\} + \mathrm{E}\{L_{22}\mathbf{r}\} \\ &= \frac{1}{n}\sum_{i=1}^{n}\sum_{j=1}^{N} C_{12,ij}\alpha_j \\ &= \bar{\mathbf{c}}^T\boldsymbol{\alpha} = \bar{\mathbf{c}}^T C_{11}^{-1}\mathbf{y} \quad \square \end{aligned} \tag{7}$$

$$\begin{aligned} \mathrm{Var}\{\mathrm{E}\{\mathbf{y}_s\}\} &= \mathbf{d}^T\left[C_{22} - C_{12}^T C_{11}^{-1} C_{12}\right]\mathbf{d} \\ &= \mathbf{d}^T C_{22}\mathbf{d} - \mathbf{d}^T C_{12}^T C_{11}^{-1} C_{12}\mathbf{d} \\ &= \bar{C}(V,V) - \bar{\mathbf{c}}^T C_{11}^{-1}\bar{\mathbf{c}} \\ &= \bar{C}(V,V) - \boldsymbol{\lambda}^T\bar{\mathbf{c}} \quad \square \end{aligned} \tag{8}$$

Using point scale estimates is therefore consistent with geostatistical scaling theory under conditions when that theory is applicable. Averaging a set of point scale values accounts for scale and shape as the average covariance approach does. Although this discussion has shown that unstructured grid volumes can be accounted for, it has not given any indication for integrating multiscale sample data such as core, log and seismic. An issue that has been resolved is that integration of these data sources is only necessary at a points scale and not at the range of scales presented by unstructured grids.

Convergence

In the context of this paper, convergence defines how numerical upscaling approaches compare with the theoretically correct result. It assesses how the error between them changes with the degree of refinement of unstructured grid elements. Several upscaling approaches are analyzed: arithmetic averaging for continuous variables such as porosity, for categorical variables such as facies, and for non-linear averaging variables such as permeability. Refinement is assumed to be tetrahedralization or triangulation, although similar equations would result using other conforming methods. Gaussian simulation is used to populate the barycentres at a point scale.

First, define the partition of an unstructured element *V* into a set of *n* tetrahedra *T*: $t_k \in T, k = 1,\ldots,n$. The volume of each tetrahedron is Δt_k with barycentres at x_k. All variables to be considered are random and specified by random field models $Z(x)$ which are defined for all *x*. Theoretical and numerical values for arithmetic averaging variables have already been defined by (1) and (2) respectively. Computing an arithmetic average of a random field under conditions mentioned in the first paragraph is equivalent to a Riemann sum and the convergence is defined by (9), which if normalized by the volume of *V* is the arithmetic average. Note that in the limit as Δt approaches zero *n* approaches infinity. The discretization error ε for *T* is defined by (10) and using the modulus of continuity of $Z(x)$ defined by (11) the error bound is given by (12). In (11), *s* is a spatial location, $\mathrm{d}(s, x_k)$ is the distance between *s* and x_k and *h* is the largest observed distance between a barycentre and its associated tetrahedron vertices. It is a measure of the continuity of the random field $Z(x)$.

$$\lim_{\Delta t \to 0} \sum_{k=1}^{n} Z(x_k)\Delta t_k = \int_V Z(x)dx \tag{9}$$

$$\varepsilon = \frac{1}{V}\left| \int_V Z(x)dx - \sum_{k=1}^{n} Z(x_k)\Delta t_k \right| \tag{10}$$

$$\omega_Z\left(x_k;h\right) = \sup_{s:\mathrm{d}(s,x_k)\le h} \left|Z(s) - Z(x_k)\right| \tag{11}$$

$$\left| \int_V Z(x)dx - \sum_{k=1}^{n} Z(x_k)\Delta t_k \right| \le V \cdot \omega_Z\left(x;h\right) \tag{12}$$

Evaluating the error bound is complex for several reasons: sampling the random field at $Z(s)$ depends on the values already evaluated at $Z(x_k)$, k=1,…,n through the covariance function of Z; all $Z(s)$ are associated with conditional distributions and the modulus of continuity must be evaluated in expected value; and if multiple facies and variables are considered, the conditional distributions of $Z(s)$ become quite complex and difficult to specify analytically. Despite this, one conclusion that can be drawn from these equations is: random fields with more spatial correlation, especially at the short range within Δt_k, will have a lower modulus of continuity resulting in a lower error bound permitting coarser refinements.

Difficulties in evaluating the error bound warrant a numerical investigation into the convergence of point scale averages. To consider random fields with uncertainty, the error in (10) will be evaluated without taking the absolute value, so the expected value and variance should approach zero as n approaches infinity. The exact value of the integral in (10) is approximated by using a large number of discretization points. Due to its complexity, permeability is evaluated first with regular grids. Following this will be an assessment of convergence for Gaussian fields, porosity and facies on PEBI grid elements discretized into triangles and tetrahedra.

Permeability

Convergence properties of permeability are challenging to analyze since it does not average arithmetically. Describing the flow through volume V to match the flow through it at a higher resolution is accomplished with a permeability tensor derived using flow based upscaling. Several procedures for this exist and each will have different convergence properties.

A single phase extended local upscaling process is used to evaluate the convergence of the following quantities for upscaling permeability: mean pressure gradient over V; mean flux through V; and tensor components. Permeability is assumed a scalar quantity at the point scale, $Z(x)$. In the extended local upscaling procedure, a set of fine scale permeabilities that cover the coarse volume plus some additional surrounding coarse volumes are chosen as the local domain, Figure 3. General boundary conditions (BC) are applied in the principal coordinate directions to provide a set of Darcy equations from which a permeability tensor can be computed.

Darcy's law is often expressed as (13), where K is the hydraulic conductivity tensor, ∇p is the pressure gradient, and **q** is the flux. In two dimensions, performing one solve with general boundary conditions in the x direction and a second solve with them in the y direction provides four equations for the upscaled tensor components to be derived from (14), where q_x^x and q_y^x are the mean flux in x and y due to the general BC in x (similarly for q_x^y and q_y^y), $\nabla\overline{p}_x^{\,x}$ and $\nabla\overline{p}_y^{\,x}$ are the mean pressure gradient in x and y due to general BC in x (similarly for $\nabla\overline{p}_x^{\,y}$ and $\nabla\overline{p}_y^{\,y}$), and $\overline{K}_{xx}$, $\overline{K}_{xy}$, and $\overline{K}_{yy}$ are the components of the assumed symmetric positive definite upscaled permeability tensor. Equation (14) can be reformatted as a linear programming problem that must be solved for $\overline{K} \ge 0$ (15), which is similarly expressed in three dimensions. An additional error is introduced, that being the residuals between the true flux through V and those predicted by regression. This is a measure of the information lost in increasing scale.

$$\mathbf{q} = -K\nabla p \tag{13}$$

$$\begin{aligned} q_x^x &= -\left[\bar{K}_{xx}\nabla\bar{p}_x^x + \bar{K}_{xy}\nabla\bar{p}_y^x\right] \\ q_y^x &= -\left[\bar{K}_{xy}\nabla\bar{p}_x^x + \bar{K}_{yy}\nabla\bar{p}_y^x\right] \\ q_x^y &= -\left[\bar{K}_{xx}\nabla\bar{p}_x^y + \bar{K}_{xy}\nabla\bar{p}_y^y\right] \\ q_y^y &= -\left[\bar{K}_{xy}\nabla\bar{p}_x^y + \bar{K}_{yy}\nabla\bar{p}_y^y\right] \end{aligned} \qquad (14)$$

$$\begin{bmatrix} \nabla\bar{p}_x^x & \nabla\bar{p}_y^x & 0 \\ 0 & \nabla\bar{p}_x^x & \nabla\bar{p}_y^x \\ \nabla\bar{p}_x^y & \nabla\bar{p}_y^y & 0 \\ 0 & \nabla\bar{p}_x^y & \nabla\bar{p}_y^y \end{bmatrix} \begin{bmatrix} \bar{K}_{xx} \\ \bar{K}_{xy} \\ \bar{K}_{yy} \end{bmatrix} = \begin{bmatrix} q_x^x \\ q_y^x \\ q_x^y \\ q_y^y \end{bmatrix} \quad \text{s.t.} \quad \bar{K} \geq 0 \qquad (15)$$

Upscaling studies were conducted in two dimensions using a 10 by 10 volume that was surrounded by 8 others of equal size and all were discretized into 961 points (8649 total) to compute the actual permeability tensor. A spherical variogram with no nugget effect and a range of 5*V* was used. Gaussian fields were transformed to be lognormal to represent a permeability field according to $Z(x) = \exp\left(3Y(x)\right)$, where *Y*(*x*) is the Gaussian field and *Z*(*x*) is the permeability field in millidarcies. Three realizations and the resulting permeability tensors using all 961 points are shown in Figure 4.

Error curves for the mean pressure gradient, mean flux, and tensor components were standardized by the approximated actual values. These error curves are shown in Figure 5 followed by the error curves of the tensor components and residuals in Figure 6 and Figure 7. Even though the errors are not necessarily Gaussian, confidence intervals were still calculated and they do appear to provide meaningful bounds. Because pressure, flux, and permeability are all tied via (13), they show similar convergence characteristics, which are surprisingly not much different than those of Gaussian fields covered in the next section. Equation (13) also ties the errors: an error of 5% in tensor permeability components corresponds to an error of 5% in flux. Flux residual curves in Figure 7 indicate several permeability fields that have very slow convergence of error. These realizations are identified in Figure 8. Realizations that are more or less homogeneous show low residuals; those with moderate permeability ranges that are somewhat heterogeneous show higher residuals; and those realizations with large ranges and/or a high degree of heterogeneity result in the highest residuals. As a side comment, this highlights the importance of segregating high permeability contrasts for grid design and upscaling purposes.

Analyzing an effective range of variograms and reservoir conditions to observe the convergence properties of the various upscaling techniques is a futile exercise, especially when nothing about grid design has been considered. Apparent convergent rates are lower than actual due to unreasonable mixing of permeability within the same volume. A practical approach to determining the discretization parameters will be project dependent, and this requires further development.

Convergence with unstructured grids

Carrying out convergence studies is difficult in the unstructured case due to reasons of geometry and flexibility. Partitioning a volume into triangles or tetrahedra, then refining or coarsening that result to assess changes in error is not straightforward. Additionally, there are no rules for how or where to refine a volume, which may prove useful in maximizing the convergence rate of volume estimates to the true value for any given realization. However, examples will be given for convergence of Gaussian field and facies in two dimensions and porosity in three dimensions. Triangulation and tetrahedralization are well developed techniques and existing programs are available: *Triangle*, by Shewchuk (1996) and *TetGen* by Si (2006) from the Numerical Mathematics and Scientific Computing Research Group. Both are quality mesh generators and parameters that control the volume and angles of resulting elements are used to control mesh refinement for the convergence studies.

Convergence of triangulated volumes is assessed by generating random polygonal regions that fit within a 10 by 10 window, refining them with a large number of triangles to obtain an estimate of the true value, and then exploring a number of coarser triangulations to obtain error curves. Element size is constrained by a maximum area parameter and the shape is constrained by an interior angle parameter of 30 degrees. This prevents triangles with high aspect ratios from being formed, which tend to cause poor performance for both numerical integration and flow simulation.

An example was setup using a spherical variogram with ranges of *V*/2, *V*, and 5*V* where *V* is assigned a value of 10. A random polygon was created and discretized into 1114 triangles that corresponds to an area constraint of 0.1, Figure 9. Area constraints were varied from 20 to 0.5 to construct the error curves, and for this polygon the resulting triangulations ranged from 7 to 221

elements. These numbers are fairly consistent with the discretization used for the permeability case. Resulting error curves and confidence intervals are shown in Figure 10. A slightly wider confidence interval is observed due to the irregular partitioning: it seems triangulation, when used as a midpoint integration rule, is not as efficient as a perfect regular grid partitioning for Gaussian random fields. However, it is not possible to discretize arbitrary polygons with a conforming regular grid, which adds a significant degree of difficulty for upscaling permeability. Error curves were also generated for facies using a spherical variogram with range 5*V* and three facies with proportions 0.2, 0.3, and 0.5, Figure 11.

Two types of unstructured volumes were explored in 3-D: those from 2.5D grids and fully unstructured perpendicular bisector or Voronoi cells. For the 2.5D case, the unstructured cell was discretized into 4400 tetrahedra to approximate the true average. A spherical variogram with ranges *V*/2, *V*, and 5*V* was used, where *V* is equal to 10. Convergence results for a Gaussian field are shown in Figure 12. One realization from the 5*V* range case is shown in Figure 13, along with one realization for a voronoi cell. Convergence of errors for these two types of volumes showed no significant differences and only the 2.5D results are shown.

Three studies were also done using the porosity distribution shown in Figure 14. Spherical variograms with range *V*/2, *V*, and *V* with a 20% nugget effect are used, Figure 15. The errors and confidence intervals are much smaller than before due to the reduced variance of porosity.

Conclusions

Extending geostatistics to populate unstructured grids has several requirements. This paper discussed admissible discretization, which involves refining an unstructured grid into a set of finer scale elements so that upscaling can be achieved. In most cases, permeability is the limiting variable and upscaling requires a mesh that is applicable to current flow simulation methods. Tetrahedral refinement is one promising option. Also explored was the concept of scale. The only scales of concern are the refinement points and the usual core, log, seismic, and production data. Lastly, the convergence of upscaling methods for permeability, facies, porosity, and Gaussian random fields was analyzed. For arithmetic averaging, the major contributors that effect the error variance are the variogram and the distribution. Larger variogram range leads to faster convergence; a nugget effect slows convergence; and lower errors occur for distributions that have a small finite range as compared to a Gaussian distribution which has an infinite range. Flow based upscaling was also explored, and results were comparable to those for arithmetic averaging. Larger residuals occur from combining high permeability contrasts and heterogeneity within a volume being upscaled. Arithmetic upscaling processes were explored on unstructured grid elements. Discretization was accomplished with triangulation and tetrahedralization: they are well developed techniques; conforming grids are possible with any volume, which is a nice result for upscaling purposes; and triangular and tetrahedral elements are applicable to mixed finite element and multi point flux simulation schemes. Resulting convergence of errors did not indicate any bias with arithmetic averaging.

If geostatistical tools are to be extended to characterize unstructured grids, a method of selecting discretization parameters must be available. Error convergence studies indicated relationships between the volume, variogram, and distribution function of reservoir properties. The potential complexity of these, along with the geometry of unstructured grids makes the selection of discretization parameters complex and this is addressed in future research.

References

Leuangthong O. (2004) The promises and pitfalls of direction simulation. Centre for Computational Geostatistics, Report 6, paper 103

Manchuk J., Leuangthong O., and Deutsch C.V. (2004) Direct geostatistical simulation on unstructured grids. Centre for Computational Geostatistics, Report 6, paper 101

Pyrcz M.J. and Deutsch C.V. (2002) Building blocks for direction sequential simulation on unstructured grids. Centre for Computational Geostatistics, Report 4

Shewchuk JR (1996) Triangle: Engineering a 2D Quality Mesh Generator and Delaunay Triangulator. In Applied Computational Geometry: Towards Geometric Engineering (Ming C. Lin and Dinesh Manocha, eds.), vol. 1148 of Lecture Notes in Computer Science, 203-222, Springer-Verlag, Berlin.

Si H (2006) TetGen: A quality tetrahedral mesh generator and three-dimensional Delaunay triangulator. Numerical Mathematics and Scientific Computing Research Group, Weierstrass Institute for Applied Analysis and Stochastics

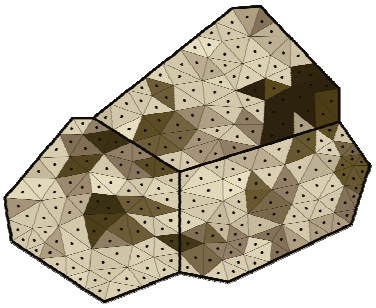

Figure 1: Random estimates generated at barycentres. Coarse lines are the unstructured grid elements, fine lines are the refinement, and bullets define the barycentres

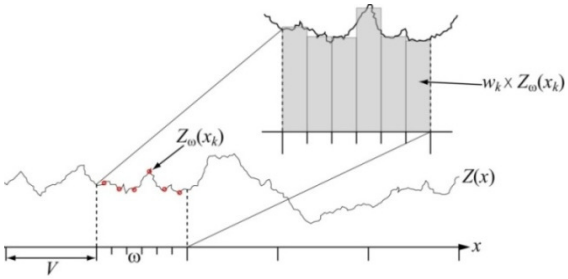

Figure 2: Numerical regularization of a random field via the midpoint rule

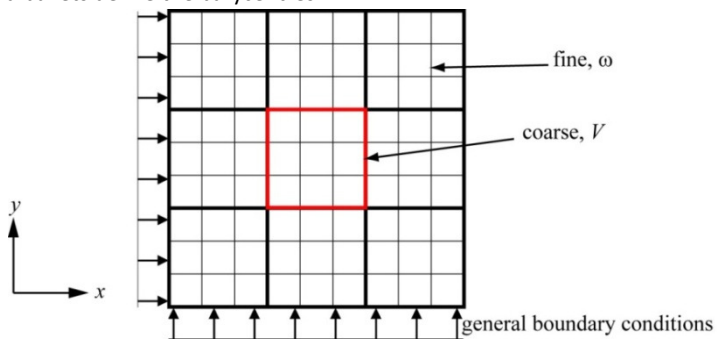

Figure 3: Extended local upscaling grids

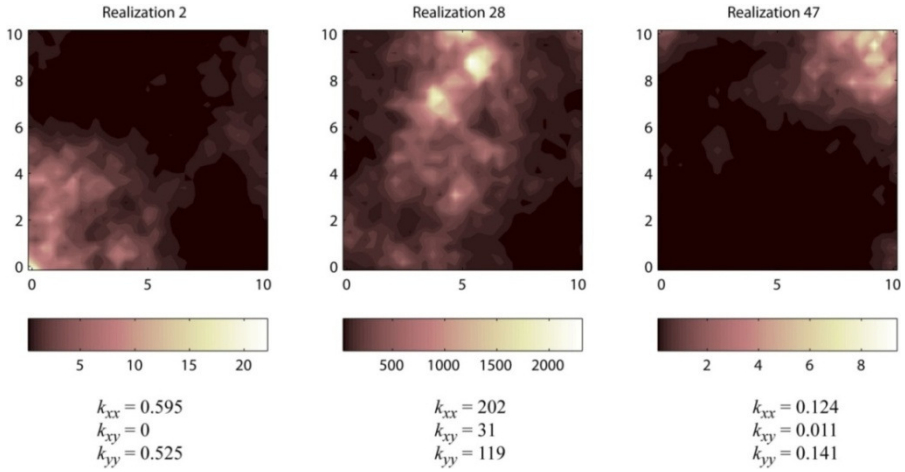

Figure 4: Permeability fields within *V* and resulting tensors

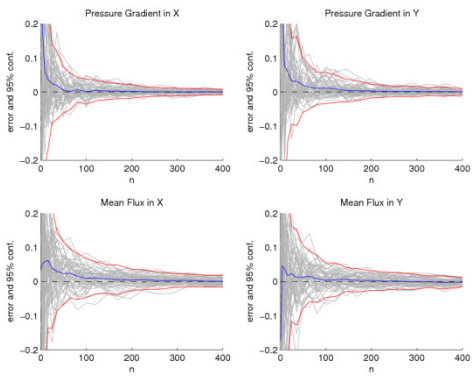

Figure 5: Pressure and flux errors for spherical range of 5*V*

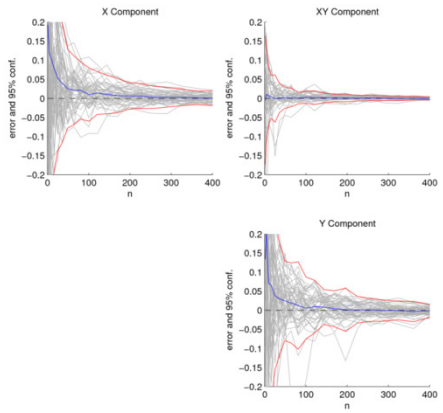

Figure 6: Permeability tensor component errors

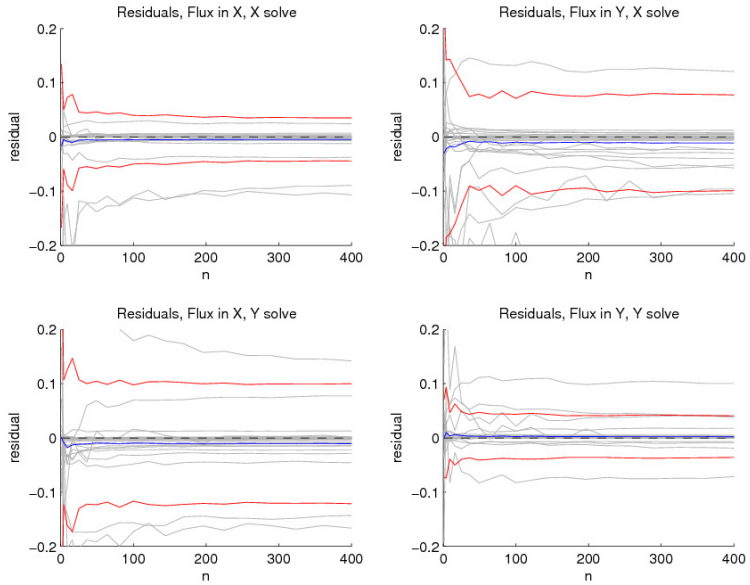

Figure 7: Flux residuals resulting from scale change

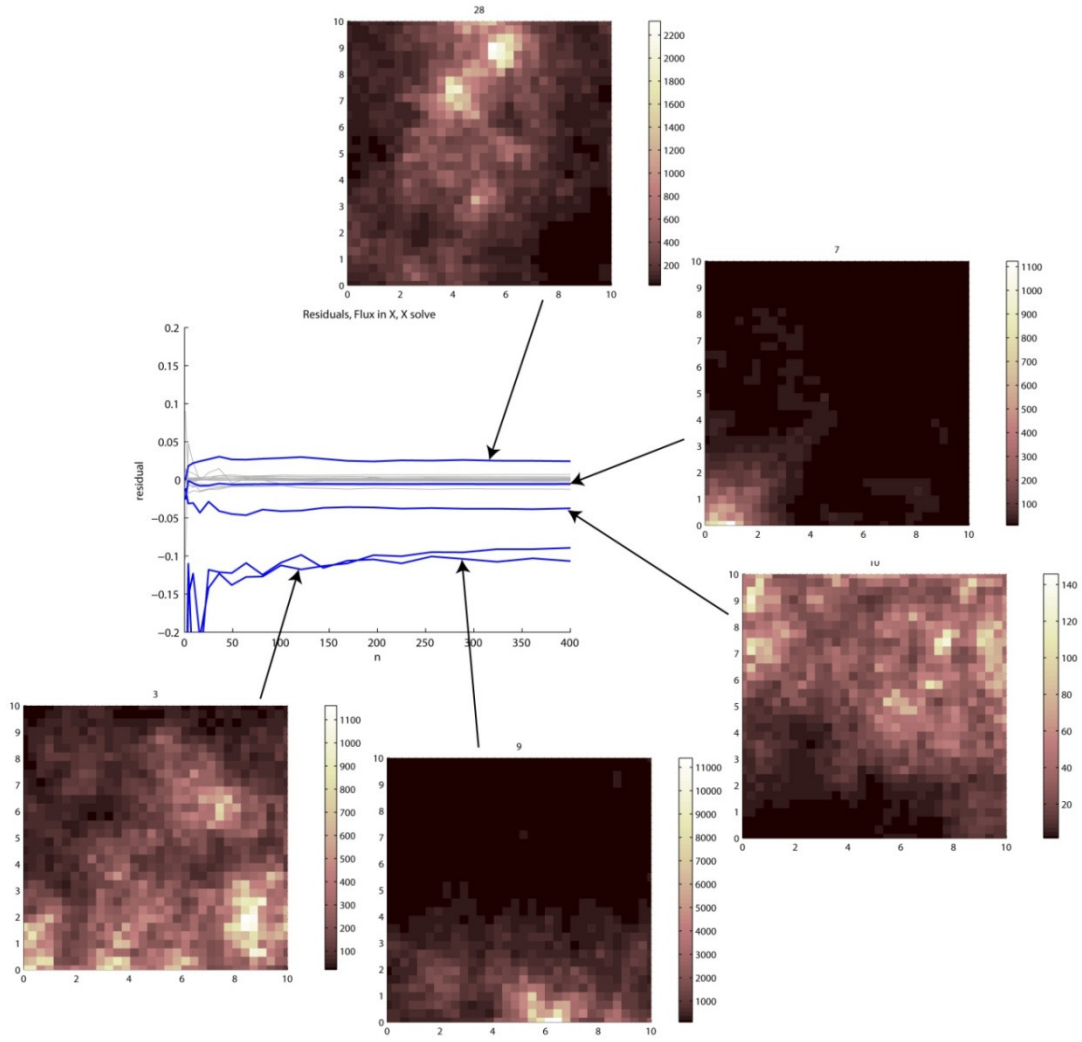

Figure 8: Flux residual curves and associated permeability fields

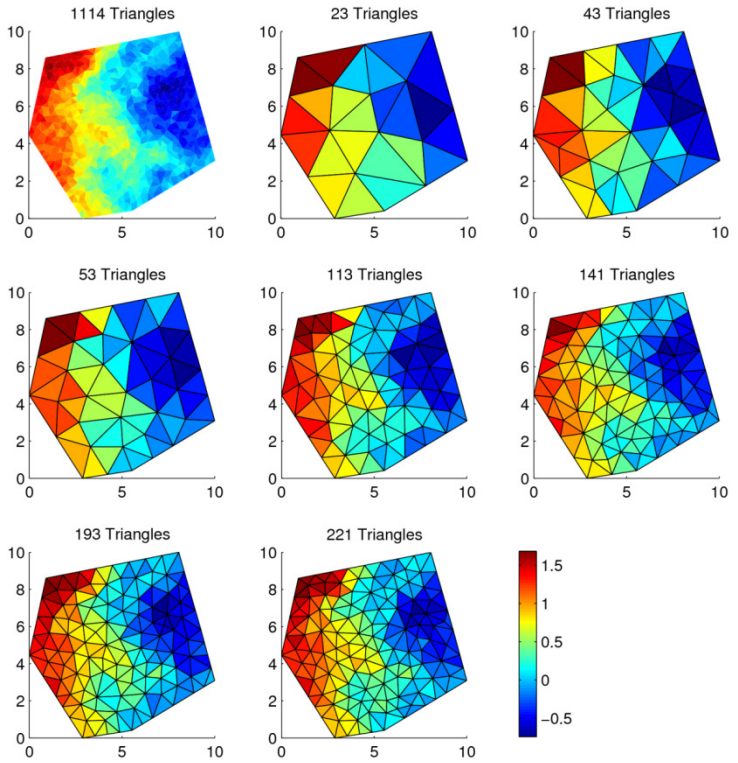

Figure 9: Example polygon and various refinements

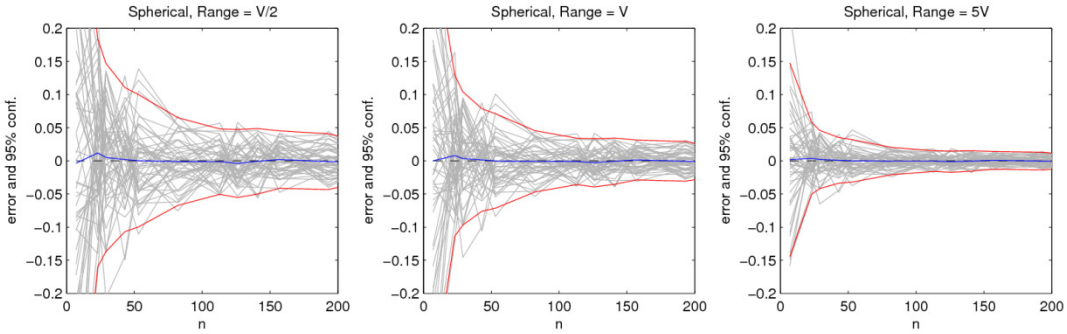

Figure 10: Convergence studies using triangulation and spherical variograms in two dimensions

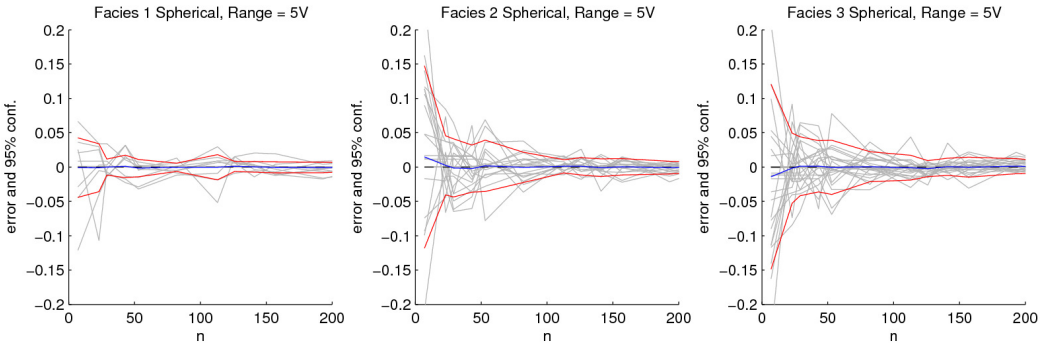

Figure 11: Convergence study for facies using triangulation and spherical variograms in two dimensions

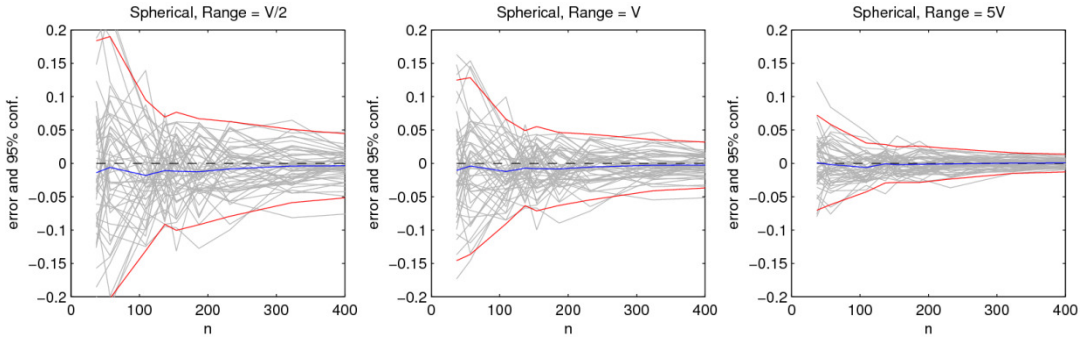

Figure 12: Convergence studies using tetrahedra and spherical variograms in three dimensions

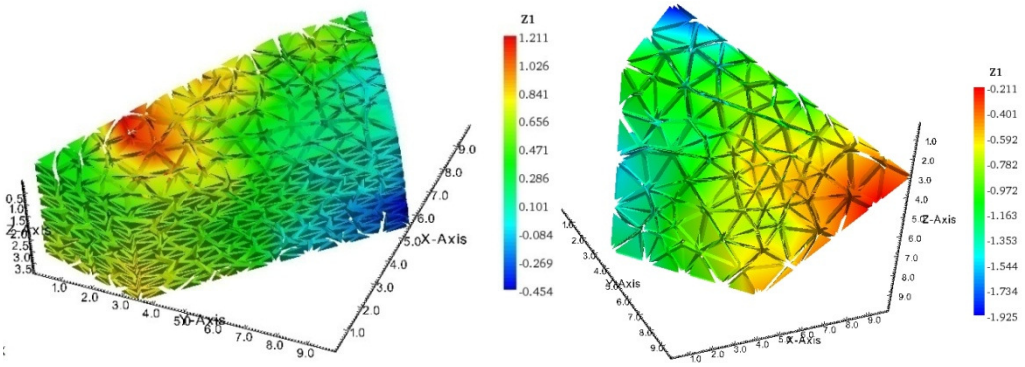

Figure 13: Isometric view of 2.5D grid cell (left) and voronoi cell (right) shaded with a Gaussian random field. Cells are refined into tetrahedra that are reduced to show detail.

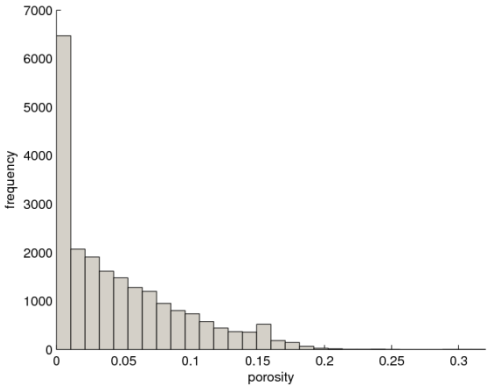

Figure 14: Porosity histogram

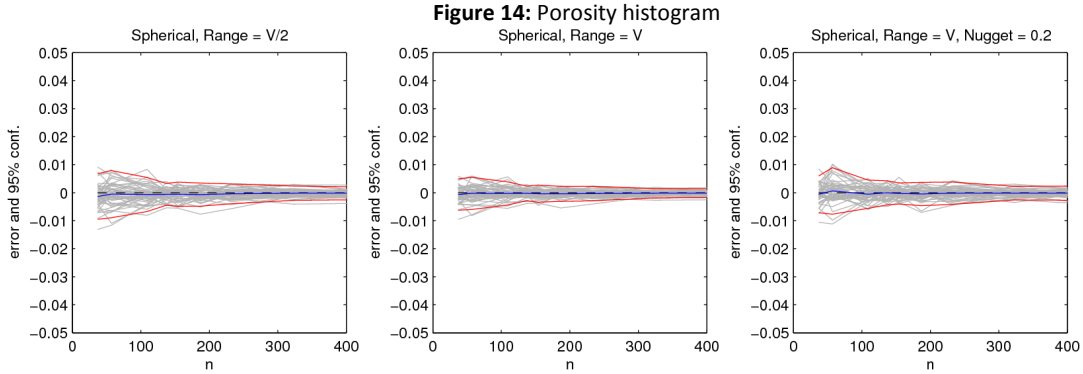

Figure 15: Convergence of porosity using tetrahedra and various spherical variograms